Journal of Applied Polymer Science

Elastomer Composite Based on EPDM Reinforced with Polyaniline Coated Curauá Fibers Prepared by Mechanical Mixing

Joyce R. Araujo,[1] Cristina B. Adamo,[2] Werickson F. C. Rocha,[1] Marcos V. Costa e Silva,[1] Vitor Carozo,[1,3] Vanessa L. Calil,[1] Marco-A. De Paoli[2]

[1]Divisão de Metrologia de Materiais, Instituto Nacional de Metrologia, Qualidade e Tecnologia (Inmetro), 25250-020 Duque de Caxias, Rio de Janeiro, Brazil

[2]Instituto de Química, Unicamp C.P. 6154, 13083-970 Campinas, São Paulo, Brazil

[3]Departamento de Engenharia Metalúrgica e de Materiais, Universidade Federal do Rio de Janeiro, 21941-972, Rio de Janeiro, Brazil

Correspondence to: J.R. Araujo (E-mail: jraraujo@inmetro.gov.br)

ABSTRACT: Curauá fibers were used to reinforce elastomeric matrices with polyaniline (PAni) synthesized directly on the fiber surfaces to produce antistatic-reinforced composites. In this work, composites of poly(ethylene-*co*-propylene-*co*-diene) with curauá fibers coated with PAni were prepared by mechanical mixing in a counter-rotating twin rotor internal mixer. Then, mechanical and electrical properties of these composites were correlated to Raman and Fourier transformed infrared spectra (FTIR) using chemometric data analyze, such as principal component analysis (PCA) and hierarchical cluster analysis (HCA). Raman spectra showed correlation with electrical properties of conductive composites while FTIR spectra showed good correlation with mechanical properties. EPDM reinforced with PAni coated curauá fibers presented higher tensile strength and modulus than EPDM reinforced with pristine curauá fibers, indicating that the reinforcement effect was obtained. Chemical interaction between the phases occurs with formation of hydrogen bonding between the aminic nitrogens of PAni and the carbonyl groups of lignin of the fibers. © 2013 Wiley Periodicals, Inc. J. Appl. Polym. Sci. **2014**, *131*, 40056.

KEYWORDS: composites; conducting polymers; elastomers; fibers; spectroscopy

Received 29 July 2013; accepted 13 October 2013

DOI: 10.1002/app.40056

INTRODUCTION

Intrinsically conducting polymers, like polyaniline (PAni), are an important class of materials due to their interesting properties; electrical conductivity, electrochromism, and electroactivity.[1] Despite these advantages, its industrial use is limited because of the fragile mechanical properties of this class of polymers. Since their first preparation in 1984,[2] conductive polymer blends became the most used manner to improve the mechanical properties of conductive polymers.[3,4]

Thermoplastic elastomers, TPE, are a group of materials with high flexibility and a glass transition temperature below −20°C.[4] They can be cross-linked to provide appropriate mechanical properties, like tensile strength, modulus, and elongation.[5] These materials are commodities and have numerous applications, such as cables insulation, fuel hoses, gaskets, and several other automotive items.

The use of blends in the rubber industry is important because it allows tailoring of the characteristics of a material by using in their composition two or more polymers with different properties.[6–9] Poly(ethylene-*co*-propylene-*co*-ethylidenenorbornene), EPDM rubber, was chosen in this work because of its highly saturated structure affording a material with good resistance against weathering.[10] PAni is one of the most studied conducting polymers due to its high electrical conductivity associated to good stability, facility of preparation, and low cost of the monomer.[11,12] Direct deposition of PAni on a vegetable fiber surface and its use as reinforcement of a thermoplastic material is an efficient way to generate antistatic-reinforced composites.[13–15]

The first work (1986) about preparation and characterization of composites based in conducting polymers and cellulose materials was realized by Bjorklund and Lundstrom[16] that described the synthesis of methylcellulose/polypyrrole composites with electrical conductivities of about 2 S cm^{-1}. After this, Bhadani et al.[17] prepared conducting natural fibers coating insulating natural fibers, such as cotton, silk, and wool with polypyrrole. The conductivities of polypyrrole coated fibers were in the range of 0.2–15 S cm^{-1} and their values show dependency with the nature of the fibers.

Experimental techniques, involving calibration methods, are employed to study the properties of polymeric materials, such as: Raman spectroscopy,[18] FTIR (Fourier transformer infrared spectroscopy), NIR (near-infrared) spectroscopy,[19] X-ray fluorescence,[20,21] time-of-flight secondary ion mass spectrometry,[22] and nuclear magnetic resonance.[23] Calibration methods were applied to polymers to study some specific properties like: degree of crystallinity,[24] additive concentrations,[25] composition of processed polymer or blend,[19] moisture content,[26] status of reaction in a reactive extrusion,[27] presence of recycled polymers,[28] and quantification of heavy metals.[29]

The presence of chemical groups in polymeric materials can be deduced using its vibrational spectra.[30] Band intensities have quantitative information about these chemical groups and a relationship between band intensities and concentration of the mixture components can be achieved using a calibration model. The most used chemometric methods to analyze spectral data of polymeric material are principal component analysis (PCA) and its quantitative models, like principal component regression (PCR) and the partial least squares (PLS) method.

In this work, composites of PAni coated curauá fibers and EPDM rubber were prepared with various PAni coated fiber contents, from 5 to 50 wt %, forming ternary phases (neat curauá fiber, EPDM matrix, and PAni). Electrical and mechanical properties of these composites were determined. They were also predicted and validated using the Raman and FTIR spectra of the starting materials and of a binary phase, PAni coated curauá fibers. We exemplify the use of the PCA and HCA multivariate analysis methods for achieving pattern recognition between samples.

Theory

According to Rocha and Nogueira,[31] multivariate methods consider simultaneously the correlation among many variables, allowing the extraction and visualization of a large amount of information. PCA is a classical data analysis method that provides a sequence of the best linear approximations to a given high-dimensional data set.[31] It is one of the most popular techniques for dimensionality reduction. The subspace modeled by PCA captures the maximum variability in the data, and can be viewed as modeling the covariance structure of the data. In PCA the data set (matrix $\boldsymbol{X}$) composed of samples (rows) and variables (columns) is decomposed into two new sets, named scores and loadings.[31–36]

Clustering is an important technique in data analysis and pattern recognition in which the objective is to try to discover underlying groupings in the data. In clustering, we try to find groups of objects as described by the data set so that objects in the same group are more similar to one another than objects in a different group. Because of this, similarity assessment and its interpretation are fundamental to the identification of the clusters. Hierarchical cluster analysis (HCA) is a method that divides a group of objects into classes in such a way that similar objects are in the same class.[31–36] As in PCA, the groups are not known prior to the mathematical analysis and no assumptions are made about the distribution of the variables. Cluster analysis searches for objects, which are close together in the variable space. As in PCA, a decision has to be made as to whether or not the data are standardized.[35] Standardizing the data will mean that all the variables are measured on a common scale so that one variable does not dominate the others. There are a number of methods for searching for clusters. In this work, Ward's method, which uses the analysis of variance approach to evaluate the distances between clusters, was used.[36]

EXPERIMENTAL

Materials

Poly(ethylene-*co*-propylene-*co*-diene), EPDM (Mangotex), aniline (Vetec, 99%), *p*-toluenesulfonic acid, *p*-TSA, (Merck, 99%), ammonium persulfate (Synth, 98%), and heptahydrated cobalt sulfate (Synth, 99%) were used in this work. The diene form present in the EPDM is 2-ethylidene-5-norbornene (ENB). Dicumyl peroxide (Sigma-Aldrich, 98%) was used as cross-linking agent for EPDM.

Curauá fibers were supplied by Embrapa-PA (Belém do Pará-Brazil), milled in a three knife rotary mill, extracted with acetone in a Soxhlet apparatus for 48 h and dried at room temperature. The extraction with acetone aims to remove impurities from the fiber surface, like waxes. After the extraction, the fibers are maintainned in acid medium for 1 h to eliminate part of lignin and promote fibrillation of the microfibrils bundles.

Preparation of PAni Coated Fibers (CF-PAni)

Before the polymerization reaction, aniline was distilled under vacuum at 130°C. The synthesis of PAni directly on the curauá fiber surface was performed based on our previous works,[13,37,38] maintaining the same monomer and oxidizing agent ratio (1 : 3). The basic experimental procedures consisted of the following steps. The commercial sample of aniline was distilled under vacuum at 130°C. The homogeneous mixture of milled fibers (300 g), an aqueous solution of *p*-toluene sulfonic acid, *p*-TSA, (1.0 mol L^{-1}), and aniline (0.1 mol L^{-1}) was formed by stirring for 1 h at room temperature. Afterwards, 2 L of an aqueous solution of oxidizing agent, $(NH_4)_2S_2O_4$ (0.3 mol L^{-1}), and *p*-TSA (1 mol L^{-1}) were added dropwise, while the mixture was kept under mechanical stirring at −5°C by pumping a cooling solution through the reactor jacket. After the color changed to dark green, the resulting mixture was removed from the reactor, filtered and washed with a 2 : 5 (v/v) water : ethanol solution.

The amount of PAni coated on the fibers was calculated using the results of CHN elemental analysis.[13] The nitrogen content in the coated samples defines the amount of PAni on the fiber. PAni content on curauá fibers calculated was equivalent to 12 wt %.

Processing of the Composites

EPDM/CF-PAni composites were prepared by mechanical mixing in an internal mixer (Haake, Rheocord-90) with counter-rotating rotors. After preliminary tests with different rotor types, the *Cam* type rotors were chosen. The processing conditions used were as follows: 80°C in the three heating zones, 50 rpm of screw rotation speed, and 6 min of mixing time.

Feeding of the mixer was done in the following sequence: EPDM, processing for 2 min, 3 wt % of dicumyl peroxide and,

at the end of the process, portions of CF-PAni (0–50 wt %). Composites were processed with 5, 10, 20, 30, 40, and 50 wt % of CF-PAni. After the thermo-mechanical processing, the molten masses were laminated in an open roll mill (MH Equipamentos) at 80°C for 15 cycles. For the vulcanization process, the laminated composites were placed in an oven at 100°C for 1 h, maintained at room temperature for 24 h and pressed for 10 min at 100°C and 16 MPa. The final laminate thicknesses were 1.50 mm and disks were cut from these using a metallic dye cutter.

Mechanical Tests

Tensile tests were performed using EMIC DL 2000 equipment, according to the DIN 53504 standard, using a crosshead speed of 200 mm min^{-1} and a cell of 500 *N*. The results are an average from at least eight samples.

Electrical Conductivity Measurements

Samples in the form of disks were coated with aluminum (3 μm thickness) and silver (2 μm thickness), forming a parallel plate capacitor. Both metals were evaporated under vacuum (2.7×10^{-6} Pa) by the physical vapor deposition process in an Angstron Engineering evaporator. Measurements were done in triplicate, according to the ASTM D-257-07 standard, in the potential range of 0–120 V, with steps of 1.0 V, in a glove box (Mbraun glove box) with N_2 as inert atmosphere (0.6 ppm of O_2).

Raman Spectroscopy

Micro-Raman scattering measurements were done using a Jobin-Ivon T64000 triple-monochromator spectrophotometer in the backscattering configuration, equipped with N_2 cooled CCD detector and a microscope with a 100× objective. The excitation laser energy was 2.41 eV (514.5 nm). The acquisition time was 40 s and the power was 5 mW.

ATR-FTIR

ATR-FTIR spectra were collected in a Perkin Elmer Spectrum GX spectrophotometer, with a ZnSe crystal. Spectra were measured with a resolution of 4 cm^{-1} and 32 scans. Samples were measured in disk form (8 mm of diameter).

Optical Microscopy

The Image J software was used to calculate the fiber lengths in the images obtained from an optical microscope (Nikon H550s) equipped with a digital camera. The images were collected using a 10 fold magnification.

Chemometric Analysis

The samples were evaluated using PCA and HCA. From the spectral results, two matrices were constructed: (10 × 3351) for data obtained by FTIR spectroscopy and (10 × 6605) for data obtained by Raman spectroscopy. The total number of rows corresponds to the number of samples and the columns correspond to the wavenumbers.

All the measured data, excluding the outliers, were evaluated at once after a mean-centering pretreatment and were submitted to the multivariate statistical analysis methods PCA and HCA using Matlab R2011b software with PLS Toolbox, version 4.21, from Eigenvector Technologies.

Table I. ATR-FTIR Peak Values and Their Assignments

	Wave number (cm^{-1})	Assignment
EPDM	2911–2850	C—H symmetric and asymmetric stretching
	1465	C—H_2 scissoring
	1375	CH_3 bending
	720	—(CH_2—CH_2) — backbone
CF	3328	O—H stretching
	2914–2852	C—H symmetric and asymmetric stretching
	1733	C=O acidic stretching
	1639	C=O aldehyde stretching
	1424	C—H aliphatic
	1030	Bending of H of ring
PAni	3369	N—H stretching
	1596	Stretching of quinoid ring
	1498	Stretching of benzenoid ring
	1300	C—N stretching/C—C bending
	1122	N—H stretching of quinone group
	813	out of plane C—H 1,4-substituted ring

RESULTS AND DISCUSSION

FTIR Spectral Analysis

Table I shows the most important bands observed in the ATR-IR spectra of EPDM [Figure 1(a)], PAni [Figure 1(b)], curauá fiber and PAni coated curauá fiber [Figure 1(c)], and composites with CF-PAni contents from 5 to 50 wt % [Figure 1(d)]. The EPDM spectrum [Figure 1(a)] exhibited characteristic bands of saturated C—H bounds: C—H symmetric and asymmetric stretching (2911 and 2850 cm^{-1}), C—H_2 scissoring (1465 cm^{-1}), CH_3 bending (1375 cm^{-1}), and —(CH_2—CH_2)— backbone (720 cm^{-1}).[39]

PAni synthesized without substrate showed the following bands [Figure 1(b)]: stretching of quinoid ring (1600 cm^{-1}), stretching of benzenoid ring (1490 cm^{-1}), C—N stretching + C—C bending (1315 cm^{-1}), C—N stretching + C—C stretching (1245 cm^{-1}) and Q=NH stretching + =Q— stretching (1100 cm^{-1}) where Q is a quinon group.[13] The curauá fiber spectrum [Figure 1(c)] showed absorption bands of chemical groups characteristic of cellulose, hemicellulose, and lignin: OH (3400–3200 cm^{-1}), C=O (1776–1715 cm^{-1}), C—O—C (1270 cm^{-1}). These are most likely composed of alkenes and aromatic groups and different oxygen-containing functional groups, like ester, ketone, and alcohol.[40] Bands assigned to PAni were observed in the CF-PAni [Figure 1(c)] spectrum at 1590 and 1460 cm^{-1}, these are characteristic of the symmetric stretching vibrational mode of the quinoid and benzenoid rings of PAni.

In the ATR-FTIR spectra of the EPDM/5CF-PAni composite [Figure 1(d)], the EPDM bands are predominant, that is, there is little difference between this spectrum and the neat matrix spectrum. In the composites with higher CF-PAni amount, 10 and

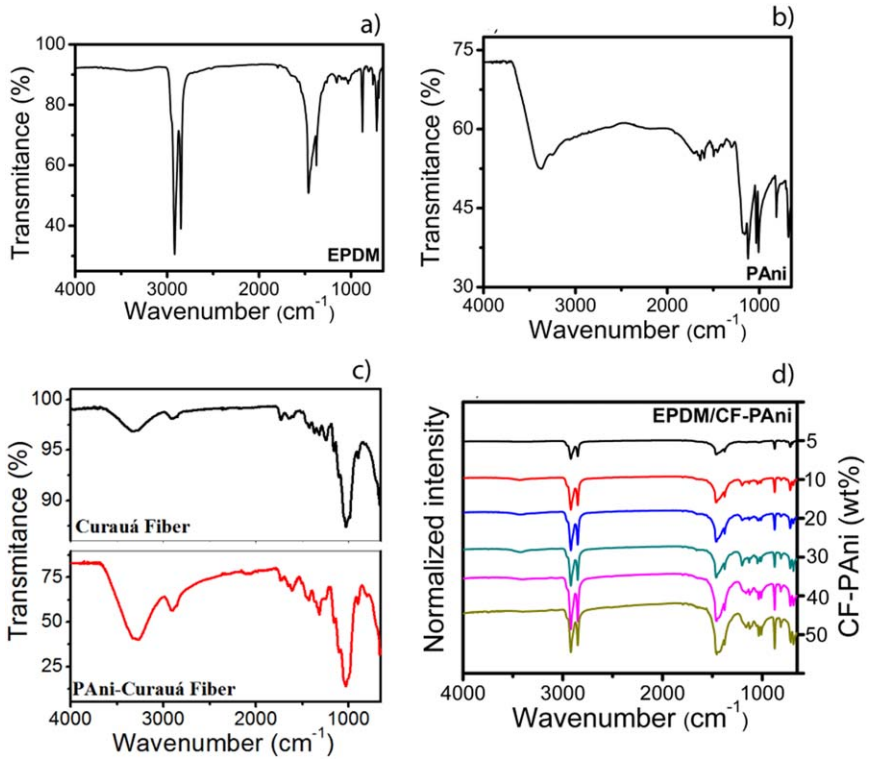

Figure 1. ATR-FTIR spectra of (a) EPDM; (b) PAni; (c) Curauá fiber and PAni coated curauá fiber; (d) EPDM/CF-PAni composites with different CF-PAni contents; from 5 to 50 wt %. [Color figure can be viewed in the online issue, which is available at wileyonlinelibrary.com.]

20 wt %, and consequently most PAni content in relation to EPDM matrix, besides the saturated carbon bands, the spectra also exhibited bands at 3429 and 1200 cm^{-1}, typical of hydrogen bonds of PAni with curauá fibers.[41] With 30, 40, and 50 wt % of CF-PAni, the bands characteristic of quinoid and benzenoid rings of PAni, at 1600 and 1500 cm^{-1}, are more intense.

Raman Spectra Analysis

Raman spectra of neat samples and mixtures were collected to compare with the spectra of the composites and to correlate the electrical and mechanical properties with the spectral data. Initially is important analyze the spectrum of the single components. EPDM is an elastomeric terpolymer from ethylene, propylene, and a nonconjugated diene. The diene comonomer used is ENB, which has two distinct types of C=C bonds, with bands at 1697 and 1577 cm^{-1}, respectively. However, during polymerization of EPDM one of the double bonds (1577 cm^{-1}) is consumed while the other (1697 cm^{-1}) remains as part of the ENB comonomer.[42] The Raman shift at 847 cm^{-1} is also assigned to the same C=C of ENB (C—H wagging), which was assigned at 833 cm^{-1} in ATR-FTIR [Figure 1(a)]. The advantage of Raman shift is that it suppresses the contribution of polar groups around the region of 1800–1500 cm^{-1}, which are normally associated with C=O, COO^{-}, H_2O, etc., and thus mainly considers the contribution from the nonpolar C=C.

In addition, in the EPDM Raman spectrum [Figure 2(a)], it is possible to observe typical stretching bands of aliphatic and aromatic C—H bonds between 3150 and 2750 cm^{-1}. The bands at 3104, 3080, 3062, and 3028 cm^{-1} correspond to aromatic stretching, while the bands at 2928 and 2852 cm^{-1} correspond to aliphatic stretching.[43,44]

Raman spectroscopic analysis of curauá fibers are presented in Figure 2(b). Its Raman shift is similar to other lignocellulosic fibers showing bands in regions characteristic of cellulose (1088 cm^{-1}) and hemicellulose (1371 cm^{-1}).[45] In addition, the main signature of lignin are strong band lines at 1603 and 1630 cm^{-1}, due to stretching of the asymmetric aryl ring.[46,47] CF-PAni spectrum [Figure 2(b)] showed higher contribution of PAni (~1500–1700 cm^{-1}) bands.

Raman spectrum of PAni [Figure 2(c)] presented sharper peaks in the region between 1000 and 2000 cm^{-1} and a broad band around 3000 cm^{-1}, together with an intense fluorescence. Fluorescence is commonly found in organic and amorphous compounds, and can many times prevent the detection of the feeble Raman bands, particularly in the visible region of the spectrum. The most intense bands in the range between 1100 and 1650 cm^{-1} corresponding to the stretching modes of the different bonds: the ring C—H bending modes between 1100 and 1210 cm^{-1}, the ring C—C stretching modes between 1520 and 1650 cm^{-1} and the different C—N stretching modes (amines, imines, and polarons) between 1210 and 1520 cm^{-1}.[48]

In the Raman spectrum of EPDM/CF-PAni composite films, Figure 2(d), a decrease in the absorption maxima at 2928 and 2852 cm^{-1} is observed and, at the same time, the appearance of the bands assigned to PAni (~1520 and 1650 cm^{-1}), with the increase of CF-PAni content (mainly in formulations containing 40 and 50 wt %).

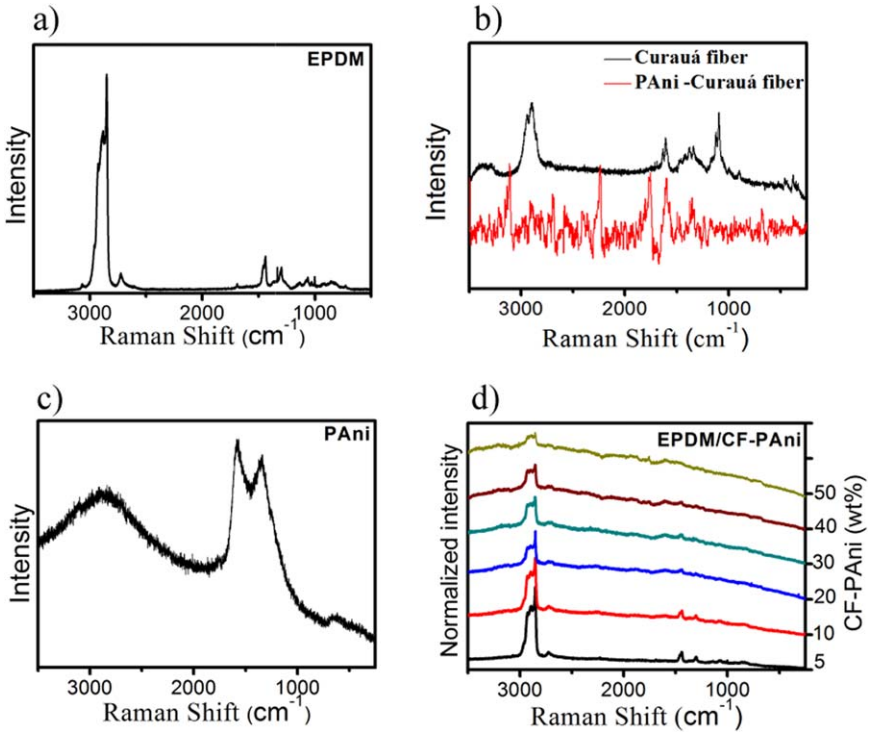

Figure 2. Raman spectra of: (a) EPDM; (b) Curauá fiber and PAni coated curauá fiber; (c) PAni; and (d) EPDM/CF-PAni composites. [Color figure can be viewed in the online issue, which is available at wileyonlinelibrary.com.]

Chemometric Analysis

Multivariate statistical analyze were used to identify similarities between the mixtures (EPDM/CF-PAni composites) and neat samples (EPDM, CF, and PAni) and to correlate spectral information with physical properties. When these statistical methods are applied, the use of all PC after decomposition of the data matrix is usually not justified.[36] Several heuristic and statistical criteria exist to decide the number of components in a PCA: percentage of explained variance, eigenvalue-one criterion, screen test, and cross-validation.[34] In this article, the cross-validation leave-one-out criterion was used. Table II shows the results of the percentage of variance explained by each PC and the cumulative variance for both models developed.

The PCA models were built using 3 PCs for both data because they explained 99.69% of **X** variance for ATR-FTIR spectroscopy data and 99.98% of **X** variance for Raman spectroscopy data (see cumulative variances in Table II), and resulted in a smaller root-mean-square error of cross-validation, which is sufficient for the construction of the PCA models.

It is possible to discriminate the studied samples through their scores plot. Figures 3 and 5 show the PCA for data obtained by ATR-FTIR spectroscopy (Figure 1) and Raman spectroscopy (Figure 2), respectively. In Figure 3 is possible to notice the distribution of binary and ternary phase samples as well as the neat species. Through this figure it is possible to visualize that the neat species (PAni, EPDM, and neat curauá fiber) are far from one another, as if they formed a triangle with vertices of PAni, EPDM, and neat curauá fiber. The binary phase sample (CF-PAni) appears together with the pure fiber (neat curauá fiber) due to the lower content of PAni (12 wt %) in relation to the fiber.

The mixtures (ternary phase samples) with higher EPDM concentration are close to the neat EPDM matrix. At lower EPDM

Table II. Percent Variance Captured by PCA Models

	Data obtained by FTIR spectroscopy			Data obtained by Raman spectroscopy		
PC[a]	Eigenvalue of cov (***X***)	Variance (%)	Cumulative variance (%)	Eigenvalue of cov (***X***)	Variance (%)	Cumulative variance (%)
1	3.80×10^5	90.27	90.27	3.29×10^{11}	98.21	98.21
2	3.64×10^4	8.65	98.91	5.16×10^9	1.54	99.74
3	3.28×10^3	0.78	99.69	5.53×10^8	0.07	99.98
4	8.73×10^2	0.21	99.90	2.44×10^8	0.07	100.00

[a] Principal components.

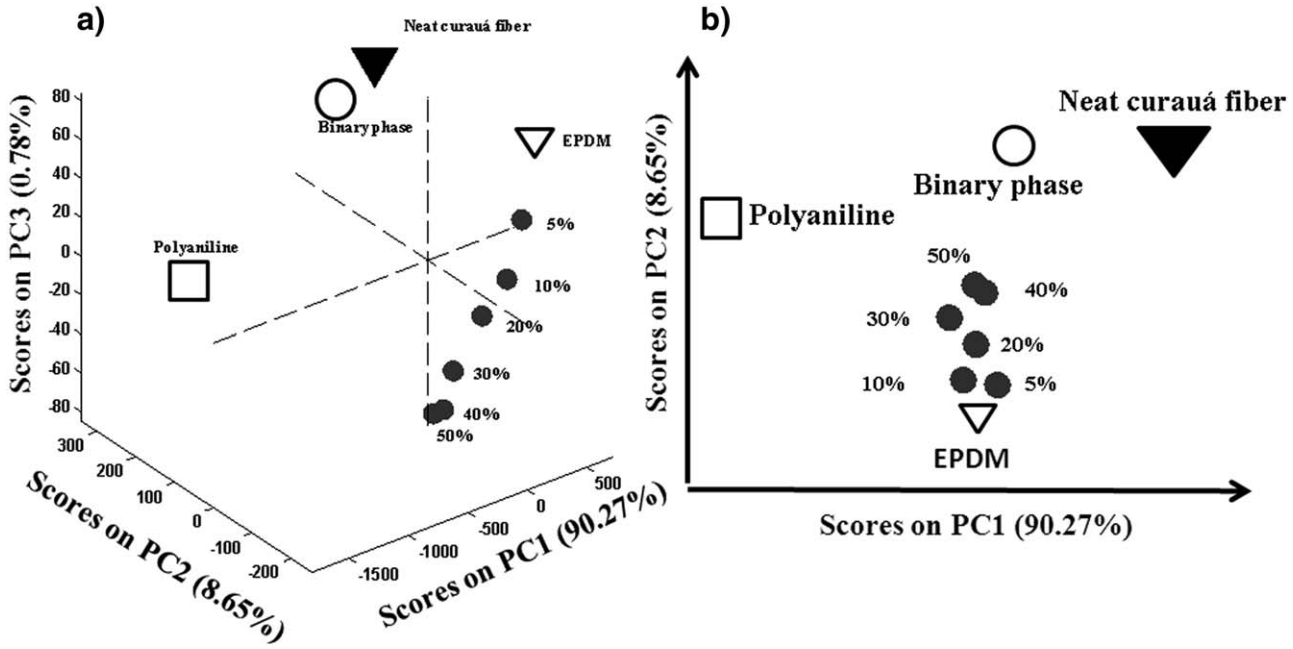

Figure 3. PCA scores plots for data obtained by ATR-FTIR spectroscopy. (a) Scores of the first three PCs. (b) Scores of the first two PCs for the data. Binary phase correspond to PAni coated curauá fiber. EPDM, PAni, and neat curauá fiber correspond to the neat species. EPDM composites with 5–50 wt % of CF-PAni correspond to the ternary phases.

concentrations, the samples move away from the EPDM matrix. In Figure 3(b) it is possible to visualize in the second PC that the composites (ternary phase samples) coming closer to the neat curauá fiber and PAni and farther from the neat EPDM matrix as the EPDM concentration is lowered, confirming that the grouping is caused by some physical property that will be evaluated latter. The same pattern obtained by PCA can be seen in the HCA dendrogram shown in Figure 4.

Figure 5 illustrates the graphical representation of PCA score plots for data obtained by Raman spectroscopy. The PC 1 component showed 98% of variance (Table II) thus, this is the component with the most Raman information. It is possible to visualize in the first principal component (PC1) more proximity between the ternary phase samples, containing 30 and 50 wt % of CF-PAni, and the PAni, whereas the ternary phase samples with 5 and 20 wt % of CF-PAni are closer to EPDM and neat curauá fibers. Ternary phases containing 10 and 40 wt % of CF-PAni are closer to the binary phase (PAni coated curauá fiber). Due to the fact that PAni is responsible for the electrical properties of polymers, it is possible to assure that the ternary phase samples, near to PAni and CF-PAni samples, are classified by the electrical property similarities, unlike the data obtained by the ATR-FTIR spectroscopy technique that are correlated to the mechanical properties.

Electrical Properties

Previous articles demonstrated that CF-PAni presents electrical conductivity in the order of 10^{-1} S cm^{-1} and pure PAni

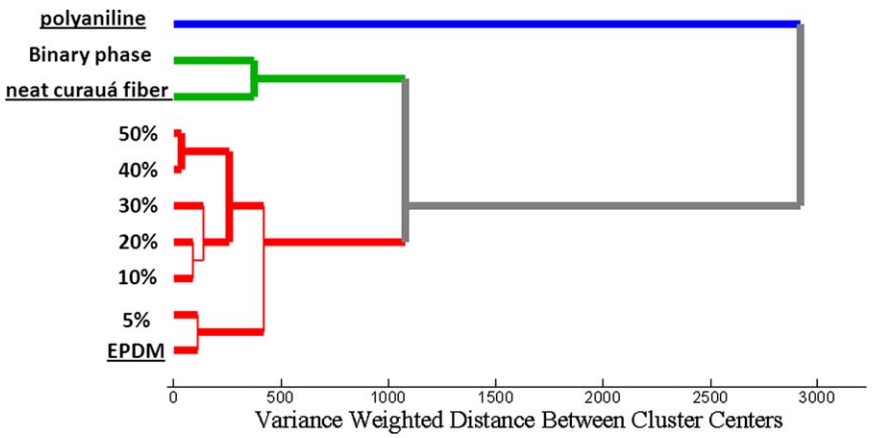

Figure 4. Dendrogram plot, resulting from HCA, for data obtained by ATR-FTIR spectroscopy and after mean-centering. [Color figure can be viewed in the online issue, which is available at wileyonlinelibrary.com.]

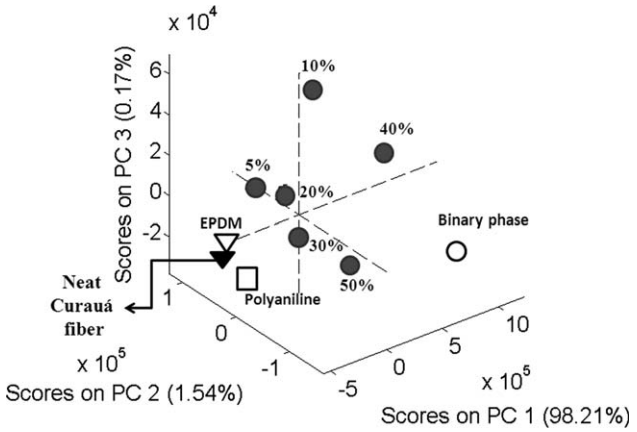

Figure 5. PCA scores of the first three PCs for the data obtained by Raman spectroscopy.

synthesized in the same conditions show 10 S cm^{-1}.[13,38] The conductivity of the PAni coated curauá fibers is lower than the conductivity of the pure PAni because the PAni nanoparticles cover only a part of the surface area of the fibers. Additionally, the presence of the curauá fibers in the polymerization reaction of PAni affects the formation of the PAni particles.[14] A recently work[49] demonstrated that PAni when synthesized directly on the fibers surface is predominantly amorphous. The transformation of crystalline PAni phase to an amorphous structure should reduce the electrical conductivity of PAni, since crystalline domains are considered the primary factors providing its high electrical conductivity.

IV-measurements [Figure 6(a)] were used to calculate the electrical properties of EPDM and its composites reinforced with CF-PAni. The conductivities of the composites were plotted in Figure 6(b) as a function of CF-PAni content. They show an increase up to 30 wt % with a consequent decrease, indicating 30 wt % as the percolation threshold. The PAni content, in relation to the total amount of EPDM and curauá fibers in the composites, is <10 wt %. In the formulations with 50, 40, 30, 20, 10, and 5 of CF-PAni, the PAni content is 6, 4.8, 3.6, 2.4, 1.2, and 0.6, respectively. The low values of conductivity may be related to the low amount of PAni in the fiber. Barra et al.[50] reported conductivities results for polystyrene-block-poly(ethylene-ran-butylene)-block-polystyrene copolymer/PAni doped with dodecylbenzenesulfonic acid (PAni.DBSA) blends, with concentrations up to 10 wt % of PAni.DBSA, of the same order of magnitude of electrical conductivities of the EPDM/CF-PAni formulations: $\sim 10^{-11}$ S cm^{-1}.

Figure 6(b) also shows the variation of tensile strength as a function of CF-PAni content and we observe that CF-PAni makes the composites more brittle, due to the intrinsic brittle character of PAni.[13–15] A similar behavior was reported for composites of nylon-6 reinforced with PAni coated curauá fibers; above a certain concentration of the filler the composites become brittle.[38] From these results, it is clear that is not possible in these composites to optimize both properties simultaneously, conductivity, and tensile strength. However, at 30 wt % of CF-PAni it is possible to reach the highest conductivity with about 50% loss in the mechanical properties of the EPDM/CF-PAni composites. At concentrations below the percolation threshold (<30 wt %), the conducting fibers are separated by layers of insulating polymer. Above the percolation threshold, the conducting fibers are in contact, forming interconnected networks.

EPDM/CF-PAni composite reinforced with 40 and 50 wt % of CF-PAni show a drop of electrical conductivity, probably due to PAni crosslinking. The electrical conductivity of the composites depends on innumerous factors related with the processing conditions, like shearing and the aspect ratio of curauá fibers after processing. High shearing during the mechanical processing, generated by high content of PAni on the fibers surface, may cause PAni degradation by crosslinking, reducing its conductivity.[51]

Mechanical Properties

Mechanical properties of the EPDM/CF and EPDM/CF-PAni composites are shown in Figure 7(a–c). The tensile strength of the composites reinforced with CF-PAni was superior to the composites reinforced with neat CF, except for the composite with 50 wt % of CF-PAni, Figure 7(a). PAni addition increases the compatibility between fiber and matrix due to hydrogen bond formation at the interface.[38] The modified fibers present better results of tensile strength in comparison to the unmodified fibers, indicating that PAni induces a stronger fiber-matrix interaction. Quinoid and benzenoid segments of PAni interact by van der Waal forces with nonpolar chains of the EPDM matrix (Figure 8) while the nitrogen atoms of PAni are

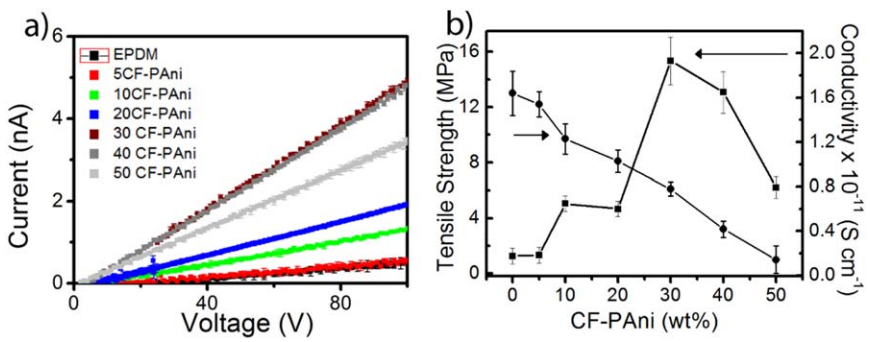

Figure 6. (a) IV (current-potential) measurements of EPDM and EPDM/CF-PAni composites and (b) Electrical conductivity and tensile strength variations of the EPDM composites as functions of CF-PAni content. [Color figure can be viewed in the online issue, which is available at wileyonlinelibrary.com.]

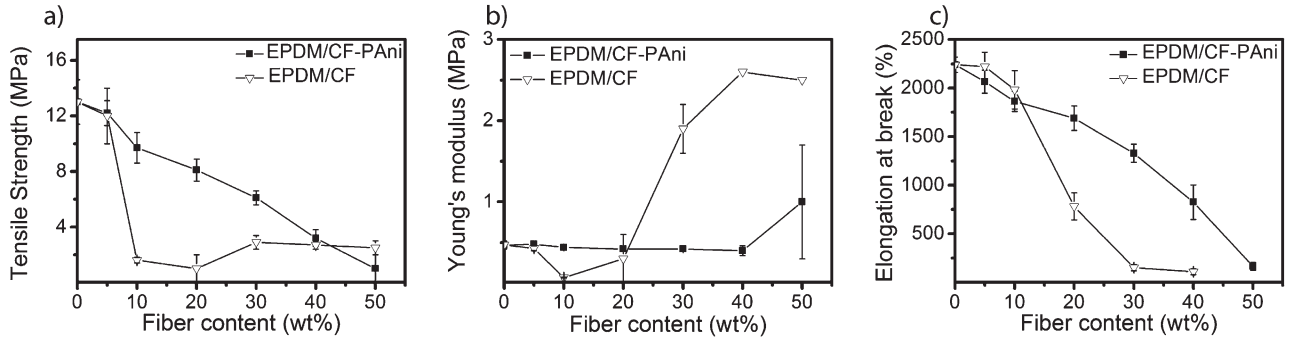

Figure 7. Mechanical properties of EPDM/CF and EPDM/CF-PAni composites. (a) Tensile strength, (b) Young's modulus, and (c) Elongation at break.

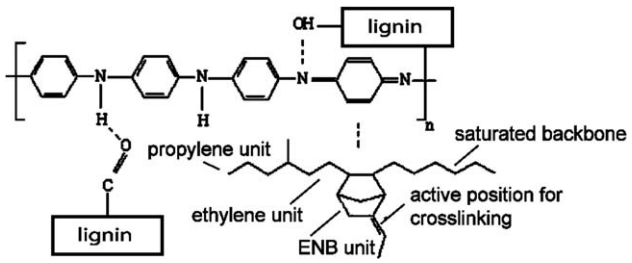

Figure 8. Illustration of the chemical interaction between the EPDM matrix, PAni, and curauá fibers.

responsible by strong interactions with curauá fiber surface, producing hydrogen bonds between aminic nitrogens and the acidic groups of lignin (carbonyl groups) and iminic nitrogens of PAni and the hydroxyl groups of the fiber surface.[52,53] The improvement in the adhesion at the interface promotes more efficient tension transfer from the matrix to the fibers, generating the reinforcement effect.

The Young's modulus of the composites reinforced with neat CF showed an improvement in relation to the EPDM matrix when the fiber content was higher than 20 wt % [Figure 7(b)], however, the composites reinforced with CF-PAni do not present an improvement of the modulus in relation to the EPDM matrix, due to the reduction of fiber length caused by PAni addition. The lower torque registered for the CF-PAni composites during mixing is an indication that a fiber length reduction occurred. The optical microscopy images shown in the next sections also corroborate this hypothesis.

Elongation decreased with the increase in CF-PAni content, Figure 7(c), as usually occurs with filled polymers, due to the

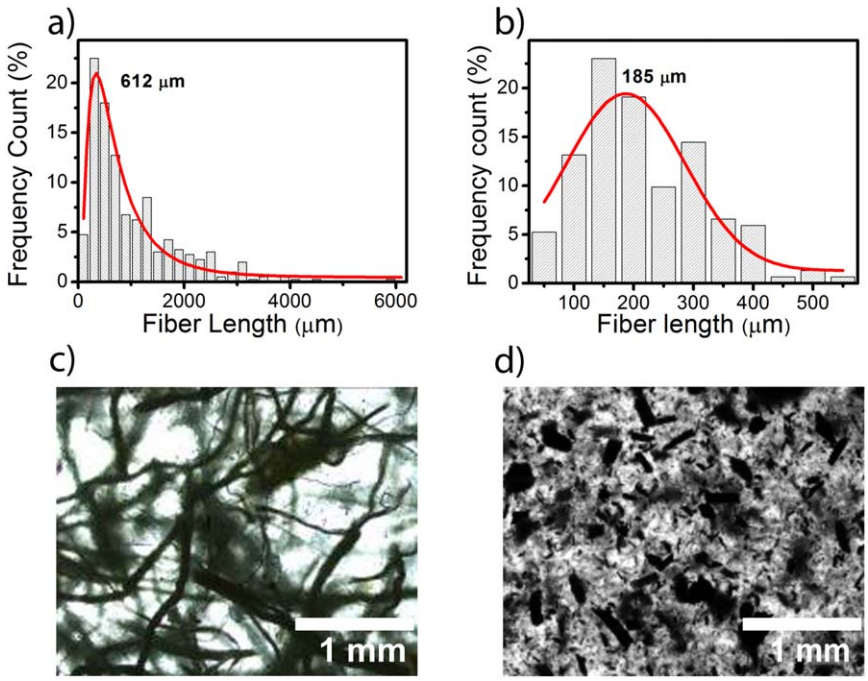

Figure 9. Length distribution of curauá fibers: (a) pristine curauá fibers, after Soxhlet extraction with acetone, and (b) curauá fibers in the EPDM composite reinforced with 5 wt % of CF-PAni. Optical microscopy images, where (c) shows a composite with 5 wt % of CF and (d) one with 5 wt % of CF-PAni. [Color figure can be viewed in the online issue, which is available at wileyonlinelibrary.com.]

immobilization of fibers adjacent to polymer segments and a possible orientation of the polymer matrix in this region.[54] These results are consistent with chemometric analysis of the ATR-FTIR spectra (Figures 3 and 4), where ternary samples with higher CF-PAni content were classified far from the neat EPDM matrix (see PC2 and PC3 scores and HCA dendogram).

Figure 9 shows the results of the fiber length measurements from the optical microscopy images. The average fiber length of the pristine curauá fibers was 612 μm [Figure 9(a)]. Processing the curauá fibers with an elastomeric matrix, like EPDM, generates shear, reducing the fiber length. This is enhanced when the fiber-matrix interactions are sufficiently good for tension transference from matrix to fiber.[55] This reduction was shown in the fiber length distribution of the composite reinforced with 5 wt % of CF-PAni [Figure 9(b)], but the broader distribution shows that the fibers in CF-PAni present higher length dispersion.

The optical micrographies [Figure 9(c,d)] show that the aspect ratio of curauá fibers in the composite reinforced with 5 wt % of CF [Figure 9(c)] was higher than in the composite with 5 wt % of CF-PAni [Figure 9(d)], and this fact is supported by the higher values of torque registered in the torque rheometer during the processing of this formulation. The higher aspect ratios of the fiber in the EPDM-CF composites are responsible also for the higher Young's modulus values. According to the "mixture law," long fibers, aligned in one direction and tested in the direction of alignment tend to reach a more rigid character and consequently have higher moduli.[56] In addition, the Young's modulus tends to change linearly with the increasing fiber content. In our present case, the fibers are not aligned and have a broad distribution of lengths. The optical micrograph of the composite reinforced with 5CF-PAni [Figure 9(d)] shows also that PAni is covering all the fibers and is well dispersed throughout the matrix, forming the percolation network interconnected by the cellulose microfibrils.

CONCLUSION

Electrical and mechanical properties of composites of an elastomeric matrix reinforced with vegetal fibers, such as curauá fibers modified with PAni, can be evaluated and predicted using spectroscopic techniques such as Raman and infrared. Spectral processing by chemometric analysis can correlate properties of neat components of the formulations with the mixtures of two or three components. This mathematical tool can be used in the quality control of processed composites on an industrial scale.

Preparation of elastomeric composites with PAni coated curauá fibers is a good way to reinforce an elastomeric material with antistatic properties. It is possible to tailor the mechanical and electrical properties of the composites by properly choosing the concentration of the modified fibers. This offers a perspective of application of this material as pressure sensor, substrate for organic devices, dosimeters of UV radiation, and electromagnetic shielding.

ACKNOWLEDGMENTS

The Authors acknowledge financial support from FAPESP (grant 2010/17804-7 and fellowship to CA process 2010/17871-6) and fellowships from CNPq. They thank Prof. Carol H. Collins for correction of the manuscript and Alexander M. Silva for the support with graphical abstract.

REFERENCES

1. Faez, R.; Gazotti, W. A.; De Paoli, M.-A. *Polymer* **1999**, *40*, 5497.
2. De Paoli, M.-A.; Waltman, R. J.; Diaz, A. R.; Bargon, J. *J. Polym. Sci. Part A: Polym. Chem.* **1985**, *23*, 1687.
3. Vallim, M. R.; Felisberti, M. I.; De Paoli, M.-A. *J. Appl. Polym. Sci.* **2000**, *75*, 677.
4. Utracki, L. A.; Favis, B. D. In Handbook of Polymer Science and Technology: Composites and Specially Applications; Ed.; Marcel Dekker Inc.: New York, **1989**; Vol. *4*, pp 183.
5. Holden G. In Understanding Thermoplastic Elastomers, E.D.; *Carl Hanser Verlag: Munich*, **2000**, Chapter *2*, pp 9.
6. Zoppi, R. A.; Felisberti, M. I.; De Paoli, M-A. *J. Polym. Sci. Part A: Polym. Chem.* **1994**, *32*, 1001.
7. Faez, R.; De Paoli, M-A. *Eur. Polym. J.* **2001**, *37*, 1139.
8. Faez, R.; Nogueira, A. F.; Carinhana, D.; De Paoli, M.-A. *Synth. Met.* **2001**, *121*, 1569.
9. Faez, R.; De Paoli, M.-A. *J. Appl. Polym. Sci.* **2001**, *82*, 1768.
10. Nandakumar, N.; Kurian, P. *Mater. Des.* **2013**, *43*, 118.
11. Sengupta, P. P.; Kar, P.; Adhikari, B. *Thin Solid Films* **2009**, *517*, 3770.
12. Shreepathi, S.; Holze, R. *Chem. Mater.* **2005**, *17*, 4078.
13. Araujo, J. R.; Adamo, C. B.; De Paoli, M.-A. *Chem. Eng. J.* **2011**, *174*, 425.
14. Souza F. G., Jr.; Picciani, P. H. S.; Rocha, E. V.; Oliveira, G. E. *Polímeros* **2010**, *20*, 377.
15. Chandran, A. S.; Narayanankutty, S. K. *Eur. Polym. J.* **2008**, *44*, 2418.
16. Bjorklund, R. B.; Liedberg, B. *J. Chem. Soc. Chem. Commun.* **1986**, 1293.
17. Bhadani, S. N.; Kumari, M.; Gupta, S. K. S.; Sahu, G. C. *J. Appl. Polym. Sci.* **1997**, *64*, 1073.
18. Lloyd, K. G.; Walls, D. J.; Wyre, J. P. *Surf. Interface Anal.* **2009**, *41*, 686.
19. Rohe, T.; Becker, W.; Krey, A.; Nagele, H.; Kolle, S.; Eisenreich, N. *J. Near Infrared Spectrosc.* **1998**, *6*, 325.
20. Ozer, E. T.; Cimenoglu, M. A.; Gucer, S. *Instrum. Sci. Technol.* **2011**, *39*, 357.
21. Pereira, F. M. V.; Pereira-Filho, E. R.; Bueno, M. I. M. S. *J. Agric. Food. Chem.* **2006**, *54*, 5723.
22. von Gradowski, M.; Wahl, M.; Forch, R.; Hilgers, H. *Surf. Interface Anal.* **2004**, *36*, 1114.
23. Momose, H.; Tomoya, M.; Hattori, K.; Hirano, T.; Ute, K. *Polym. J.* **2012**, *44*, 808.
24. Richard-Lacroix, M.; Pellerin, C. *Macromolecules* **2012**, *45*, 1946.
25. Schwarzinger, C.; Gabriel, S.; Beissmann, S.; Buchberger, W. *Mass Spectrom.* **2012**, *23*, 1120.

26. Reuvers, N. J. W.; Huinink, H. P.; Fischer, H. R.; Adan, O. C. G. *Macromolecules* **2012**, *45*, 1937.
27. Yazdani-Pedram, M.; Vega, H.; Quijada, R. *Polymer* **2001**, *42*, 4751.
28. Camacho, W.; Karlsson, S. *J. Appl. Polym. Sci.* **2002**, *85*, 321.
29. Sar, E.; Berber, H.; Asci, B.; Cankurtaran, H. *Electroanalysis* **2008**, *20*, 1533.
30. Vajna, B.; Bodzay, B.; Toldy, A.; Farkas, I.; Igricz, T.; *Marosi, Gy. Polym. Lett.* **2012**, *6*, 107.
31. Rocha, W. F. C.; Nogueira, R. *Accredit. Qual. Assur.* **2011**, *16*, 523.
32. Beebe, K. R.; Pell, R. J.; Seasholtz, M. B. In Chemometrics: A Practical Guide, Wiley: New York, **1998**.
33. Rocha, W. F. C.; Nogueira, R.; Silva, G. E. B.; Queiroz, S. M.; Sarmanho, G. F. *Microchem. J.*, **2012**, *109*, 112.
34. Martens, H.; Naes, T. In Multivariate Calibration; Wiley: New York, **1989**.
35. Brereton, R. G. In Chemometrics: Data Analysis for the Laboratory and Chemical Plant; Wiley: New York, **2003**.
36. Otto, M. In Chemometrics: Statistics and Computer Application in Analytical Chemistry; Wiley-VCH: New York, **2007**.
37. Araújo, O. A.; De Paoli, M-A. *Synth. Met.* **2009**, *159*, 1968.
38. Araujo, J. R.; Adamo, C. B.; Costa e Silva, M. V.; De Paoli, M.-A. *Polym. Compos.* **2013**, *34*, 1081.
39. Gunasekaran, S.; Natarajan, R. K.; Kala, A. *Spectrochim. Acta Part A* **2007**, *68*, 323.
40. Tomczak, F.; Satyanarayana, K. G.; Sydenstricker, T. H. D. *Compos. A* **2007**, *38*, 2227.
41. Pan, W.; Yang, S. L.; Li, G.; Jiang, J. M. *Eur. Polym. J.* **2005**, *41*, 2127.
42. Lin-Vien, D.; Colthup, N. B.; Fateley, W. G.; Grasselli, J. G. In The Handbook of Infrared and Raman Characteristics of Organic Molecules; Academic Press: New York, **1991**.
43. Mailhot, B.; Gardette, J.-L. *Vib. Spectrosc.* **1996**, *11*, 69.
44. Mitra, S.; Ghanbari-Siahkali, A.; Kingshott, P.; Hvilsted, S.; Almdal, K. *Mater. Chem. Phys.* **2006**, *98*, 248.
45. Chandel, A. K.; Antunes, F. F. A.; Anjos, V.; Bell, M. J. V.; Rodrigues, L. N.; Singh, O. V.; Rosa, C. A.; Pagnocca, F. C.; Silva, S. S. *Biotechnol. Biofuels* **2013**, *6*, 4.
46. Agarwal, U. P.; Weinstock, I. A.; Atalla, R. H. *Tappi J.* **2003**, *2*, 22.
47. Ooi, B. G.; Rambo, A. L. Hurtado, M. A. *Int. J. Mol. Sci.* **2011**, *12*, 1451.
48. Bernard, M. C.; Hugot-Le Goff, A. *Electrochim. Acta* **2006**, *52*, 595.
49. Araujo, J. R.; Adamo, C. B.; De Robertis, E.; Kuznetsov, A. Yu.; Archanjo, B. S.; Fragneaud, B.; Achete, C. A.; De Paoli, M.-A. *Compos. Sci. Technol.* **2013**, *88*, 106.
50. Barra, G. M. O.; Martins R. R.; Kafer, K. A.; Paniago, R.; Vasques C. T.; Pires A. T. N. *Polym. Test* **2008**, *27*, 886.
51. Nand, A. V.; Ray, S.; Gizdavic-Nikolaidis, G.; Travas-Sejdic, J.; Kilmartin, P. A. *Polym. Degrad. Stab.* **2011**, *96*, 2159.
52. Rodrigues, P. C.; Muraro, M.; Garcia, C. M.; Souza, G. P.; Abbate, M.; Schreiner, W. H.; Gomes, M. A. B. *Eur. Polym. J.* **2001**, *37*, 2217.
53. Benson, R. S.; Lee, M. W.; Grummitt, D. W. *Nanostruct. Mater.* **1995**, *6*, 83.
54. Iozzi, M. A.; Martins, G. S.; Martins, M. A.; Ferreira, C. F.; Job, A. E.; Mattoso L. H. C. *Polímeros* **2010**, *20*, 25.
55. Von Turkovich, R.; Erwin, L. *Polym. Eng. Sci.* **1983**, *23*, 743.
56. Bader M. G. In Handbook of Polymer-Fibre Composites, E.D.; Jones, F. R., Ed.; Longman Scientific & Technical: Essex, **1994**; pp 269–274.